CHEMISTRY OF MATERIALS

Article

pubs.acs.org/cm

Supramolecular Hydrogels Based on Glycoamphiphiles: Effect of the Disaccharide Polar Head

María J. Clemente,[†] Pilar Romero,[†] José L. Serrano,[§] Juliette Fitremann,*[,‡] and Luis Oriol*[,†]

[†]Instituto de Ciencia de Materiales de Aragón (ICMA), Universidad de Zaragoza-CSIC, Dpt. Química Orgánica, Facultad de Ciencias, Pedro Cerbuna 12, 50009 Zaragoza, Spain

[‡]Laboratoire des IMRCP, UMR CNRS 5623, Bât. 2r1, Université Paul Sabatier, 118 route de Narbonne, F-31062 Toulouse Cedex 9, France

[§]Instituto de Nanociencia de Aragón, Universidad de Zaragoza, Dpt. Química Orgánica, Facultad de Ciencias, Pedro Cerbuna 12, 50009 Zaragoza, Spain

Supporting Information

ABSTRACT: Supramolecular hydrogelators based on amphiphilic glycolipids have been prepared by clicking different sugar polar heads to a hydrophobic linear chain by copper(I)-catalyzed azide−alkyne [3 + 2] cycloaddition. The influence of the sugar polar head on the gelation properties in water has been studied, and the liquid crystalline properties of the amphiphilic materials have also been characterized. Stable hydrogels at room temperature have been obtained and the fibrillar supramolecular structures formed by the self-assembly have been studied by different microscopic techniques on the dried gel (xerogel) and hydrated conditions in order to characterize the micro- and nanostructures. Self-assembly gives rise to supramolecular ribbons with a torsion that is related to a chiral supramolecular arrangement of amphiphiles. The formation of an opposite helical arrangement of the ribbons has been found to depend on the sugar polar head. This fact was confirmed by circular dichroism (CD).

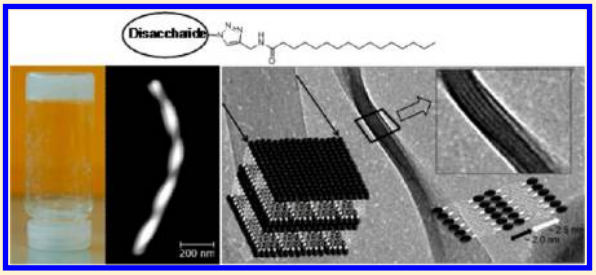

KEYWORDS: *supramolecular hydrogels, glycolipids, self-assembly, twisted ribbons, click chemistry*

INTRODUCTION

Amphiphilic molecules with a sugar polar head and a fatty hydrophobic chain can act as supramolecular hydrogelators. Supramolecular hydrogels are based on low molecular weight amphiphilic gelators that form a cross-linked network by self-aggregation, and this three-dimensional (3D) structure can trap water as solvent.[1] Self-assembly in supramolecular gels[2] occurs through a combination of noncovalent interactions such as H-bonding, $\pi-\pi$ stacking, donor−acceptor interactions, solvophobic forces, and van der Waals interactions. Taking into account the reversibility of these interactions, supramolecular gels are different from macromolecular gels because they can be cycled between free-flowing liquids and nonflowing materials by different stimuli, usually temperature, but depending on the gelator structure, the reversibility can be triggered by other stimuli like pH or irradiation.[3]

Supramolecular hydrogels are soft materials that have possible technological applications, mainly as smart materials or biomaterials. For instance, these substances have recently been described as platforms for tissue engineering and as drug delivery systems.[4] Amphihilic hydrogels based on carbohydrates have been reported as sensors[5] and as a means for cell encapsulation.[6]

The first examples of glyco-amphiphiles as hydrogelators were found in noncyclic glycosyl derivatives.[7] Conventional single-head amphiphiles[8] and bolaamphiphiles[9] were subsequently described. These compounds were reported to have the ability to gelify in a mixture of water and alcohol or, in some cases, in water alone. Carbohydrates are hydrophilic building blocks that are able to form multiple H-bonds due to the presence of hydroxyl groups, which also favor solubilization in water. Cyclic forms of carbohydrates provide more stable gels[10] because they have directional hydroxyl groups that support cooperative networks that have a self-assembled fibrous structure. Stability and gel properties are strongly dependent on the molecular structure of the gelator. The polar head of glyco-hydrogelators can be based on monosaccharides[11] and, to a lesser extent, on disaccharides.[12] The linker unit between hydrophilic and hydrophobic parts also plays a relevant role in the self-assembly. In this way, it has been reported that the presence of amide groups or the incorporation of $\pi-\pi$ stacked rings also contribute to the cooperative interactions of glyco-amphiphiles.[1,8b,9b]

Glycolipids, due to the polar asymmetry of their structure, exhibit microsegregated regions and can consequently show liquid crystal (LC) phases.[13] Thermotropic LC phases were

Received: May 16, 2012
Revised: September 17, 2012

   dx.doi.org/10.1021/cm301509v | *Chem. Mater.* XXXX, XXX, XXX−XXX

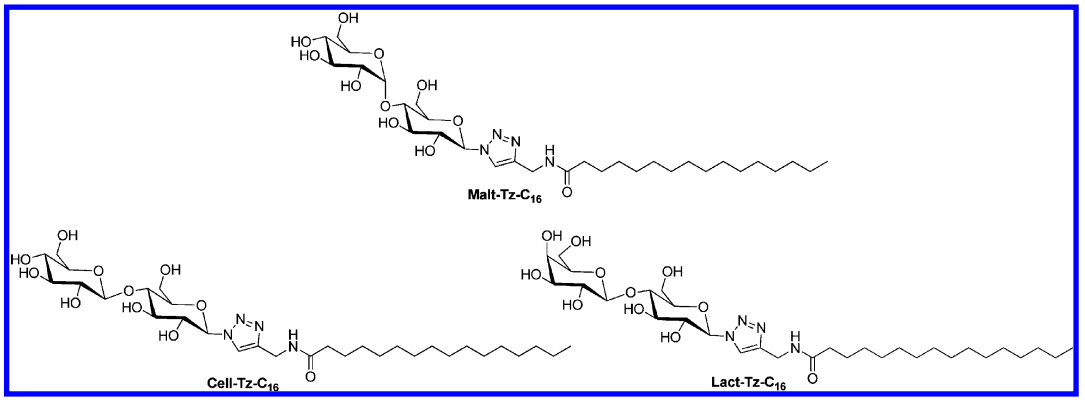

Figure 1. Chemical structure and nomenclature of the glycolipids.

first observed in alkyl glucopyranosides, and these compounds are known to form lamellar smectic phases.[14] Other mesophases, such as cubic or columnar phases, have also been reported for this sort of compound.[15] Most of the mesogenic glycolipids are based on monosaccharides,[14,16] and examples that bear a disaccharide headgroup remain relatively rare.[15,17]

In a previous study, we obtained a thermotropic maltose-based hydrogelator, Malt-Tz-C_{16} (see Figure 1), which contains a palmitic fatty chain.[18] This compound was prepared by copper(I)-catalyzed azide−alkyne [3 + 2] cycloaddition of maltosylazide and an aliphatic derivative. This click reaction[19] provides a satisfactory synthetic pathway to link parts with different polarity. The resulting triazole unit can afford a rigid fragment that impairs the free rotation of the amphiphile tail and favors the directional self-assembly in one dimension to build fibers. Moreover, this ring gives additional $\pi-\pi$ stacking, and its dipole moment increases the hydrophilicity of the amphiphile, thus aiding the gelation process more specifically in water.[1,20]

To better understand how the structure affects gel properties, in this work, we prepared two new hydrogelators based on a disaccharide. In these compounds, the stereochemistry of the sugar polar head is different to that in the maltose derivative (Figure 1). Cellobiose was selected as the sugar polar head because it has a β (1→4) connection between two glucoses instead of the α (1→4) connection of maltose. In the case of the lactose derivative, a galactose unit is located at the end of the polar head instead of glucose. In 3D, these disaccharides with different stereochemistries also adopt preferential conformations[21] that can induce different packing of the corresponding low molecular mass amphiphiles.[22] The differences in the liquid crystalline and gel-forming properties of these compounds have been analyzed. Aggregation, self-assembly, and the supramolecular gel structure were characterized by nuclear magnetic resonance (NMR), scanning electron microscopy (SEM), transmission electron microscopy (TEM), cryo-TEM, environmental scanning electron microscopy (ESEM), atomic force microscopy (AFM), and circular dichroism (CD).

RESULTS AND DISCUSSION

Synthesis of Materials. Glycoamphiphiles were synthesized by click coupling of the disaccharide polar head and the aliphatic chain, as shown in Scheme 1. The connecting group is a triazole ring bearing a neighboring amide group. The triazole ring was formed by a copper(I)-catalyzed azide−alkyne [3 + 2] cycloaddition using a disaccharide azide and N-propargylpalmitamide.

Scheme 1. Synthesis of Cell-Tz-C_{16} and Lact-Tz-C_{16}

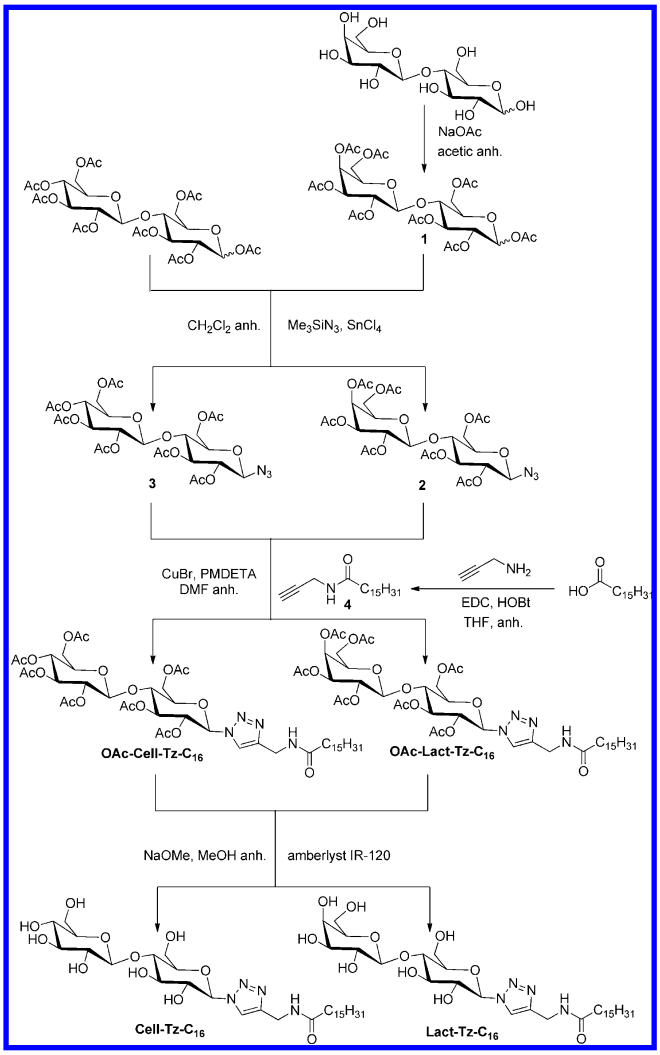

The synthesis of the disaccharide azides was performed using the corresponding peracetylated sugar as the starting material. Peracetylated lactose (**1**) was synthesized using sodium acetate and acetic anhydride, and peracetylated cellobiose was purchased. Glycosyl azides (**2**, **3**) were synthesized stereoselectively employing the general procedure described by Paulsen[23] (Scheme 1). Glycosyl azides can react through a 1,3-

dx.doi.org/10.1021/cm301509v | Chem. Mater. XXXX, XXX, XXX−XXX

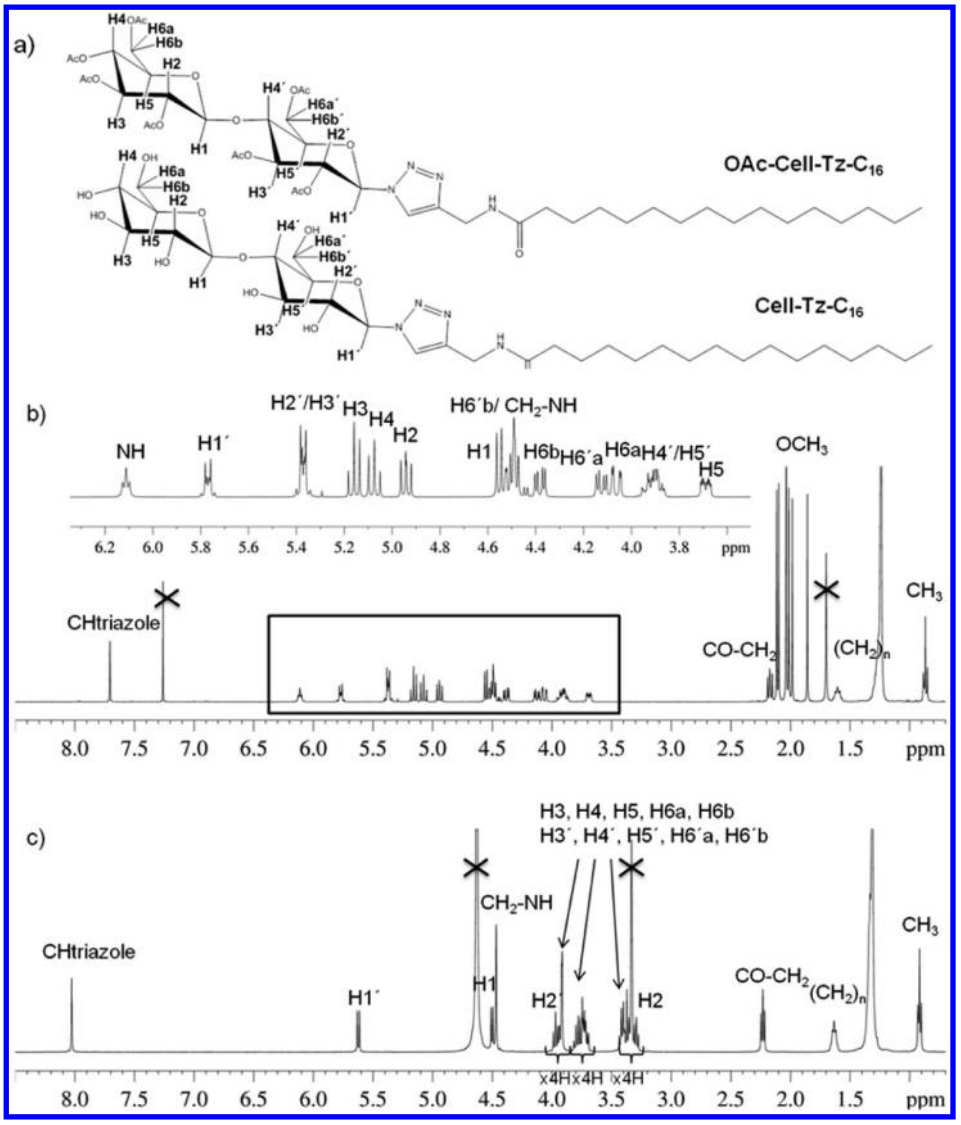

Figure 2. (a) OAc-Cell-Tz-C_{16} and Cell-Tz-C_{16} chemical structure, (b) ^{1}H NMR spectrum of OAc-Cell-Tz-C_{16} with $CDCl_3$ as solvent at 25 °C, (c) ^{1}H NMR spectrum of Cell-Tz-C_{16} with MeOD as solvent at 50 °C.

dipolar cycloaddition with N-propargylpalmitamide (**4**). The click reaction was carried out in DMF using CuBr and N-pentamethyldiethylenetriamine (PMDETA) to give the desired product. All of the protected derivatives were deacetylated at room temperature according to Zemplén's conditions (MeONa and Amberlyst IR120 in anhydrous MeOH) to give the final product in almost quantitative yield.

The peracetylated precursors and the glycoamphiphiles were fully characterized by ^{1}H and ^{13}C NMR, infrared (IR) and mass spectrometry. The ^{1}H NMR spectra of OAc-Cell-Tz-C_{16} and Cell-Tz-C_{16} are shown as representative examples in Figure 2b and c (see the Supporting Information, SI1, for the ^{1}H NMR spectra of analogs OAc-Lact-Tz-C_{16} and Lact-Tz-C_{16}). Bidimensional NMR experiments (COSY, TOCSY, NOESY, HSQC, and HMBC) were performed to corroborate the chemical structure of the glycolipids. It can be seen in Figure 3 that all of the sugar protons of OAc-Cell-Tz-C_{16} can be assigned, and these assignments are supported, for example, by TOCSY experiments. By means of correlations of a whole spin system, protons from one cycle of the sugar can be distinguished from the protons of the second cycle.

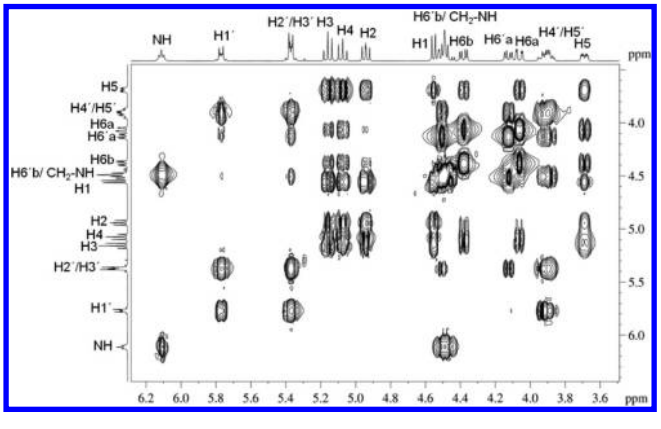

Figure 3. TOCSY spectrum of OAc-Cell-Tz-C_{16} with $CDCl_3$ as solvent at 25 °C and 60 ms of mixing time.

Liquid Crystalline Properties. Carbohydrate amphiphiles have the ability to self-assemble and undergo microphase segregation due to hydrophobic interactions of aliphatic chains and the extensive hydrogen-bonding network formed by the

dx.doi.org/10.1021/cm301509v | Chem. Mater. XXXX, XXX, XXX−XXX

polar carbohydrate heads, thus giving rise to mesomorphic properties. The behavior of these compounds and the phase transition temperatures are dependent on the nature of the carbohydrate moiety, the length of the hydrophobic alkyl chain and the type of linker between the two parts.

The mesomorphic properties of the synthesized amphiphilic glycolipids and the peracetylated precursors were studied by polarized light microscopy and differential scanning calorimetry (DSC). Thermogravimetry of samples previously dried and immediately analyzed showed that weight loss, due to a massive thermal decomposition process, is observed at temperatures above 275 °C (see the Supporting Information, SI2).

The peracetylated precursors were studied by polarized optical microscopy (POM) as a function of temperature, and mesomorphic behavior was not observed. OAc-Cell-Tz-C_{16} melts directly from a crystalline state to an isotropic liquid at 175 °C. Nevertheless, in the DSC study of OAc-Lact-Tz-C_{16}, crystallization was not observed on cooling the molten state and a glassy material was obtained. DSC traces corresponding to the second or subsequent scans only exhibit a glass transition at 52 °C (see Table 1).

Table 1. Thermal Transitions of the Synthesized Glycolipids Determined by DSC (10 °C·min^{-1})[a]

cmpd.	thermal transition (°C) [ΔH kJ/mol]		
OAc-Cell-Tz-C_{16}	Cr	175 [37.7]	I[b]
OAc-Lact-Tz-C_{16}	g	52	I[b]
Cell-Tz-C_{16}	Cr	159 [1.9][c]	S_A
Lact-Tz-C_{16}	Cr	147[1.5][c]	S_A
Malt-Tz-C_{16}	Cr 31 [2.0] Cr′ 49 [6.2][c] S_A		

[a]Results of Malt-Tz-C_{16} taken from ref 18. [b]The heating scans were carried out up to 200 °C. Data from the second heating scan. [c]The heating scans were carried out up to 165 °C to avoid decomposition. Data from the second cycle scan. Decomposition was observed in the third heating scan carried out up to 250 °C. Decomposition temperatures are around 170−175 °C. Cr = crystal, I = isotropic phase, S_A = smectic A phase, g = glassy state.

The final glycolipids Cell-Tz-C_{16} and Lact-Tz-C_{16}, as with the previously reported Malt-Tz-C_{16}, exhibited birefringent textures associated with thermotropic liquid crystalline behavior. The poorly defined birefringent textures of the viscous mesophase (see the Supporting Information, SI3) precluded unambiguous assignment of the mesophase. According to previous results obtained on maltose derivatives, it can be postulated that this mesophase is lamellar. Samples become brown due to a clear decomposition at temperatures around 250 °C.

A DSC study of the glycolipids was performed by heating the compounds to 165 °C in the first and second scans (see the Supporting Information, SI4), before decomposition in the third scan, in order to minimize thermal decomposition of the samples, which was observed in this technique around 170−175 °C. In the third scan, the sample was heated to 260 °C. Under these conditions, the second and third scans were reproducible and the transition data are gathered in Table 1.

Malt-Tz-C_{16} was previously characterized and exhibits a peak corresponding to the melting transition at around 50 °C. Above this temperature, the sample is highly viscous, and at temperatures above approximately 90 °C, the sample becomes more fluid and can be clearly characterized as liquid crystalline according to the optical observations. The decomposition temperature was detected at around 175 °C. Similar behavior was observed for Cell-Tz-C_{16} and Lact-Tz-C_{16} although the mesophase appeared at higher temperatures, around 160 and 150 °C, respectively. Textures were analogous to those observed for Malt-Tz-C_{16}. On heating samples up to 250 °C, peaks corresponding to decomposition were observed at around 170−175 °C, before isotropization.

Smectic A phase for Cell-Tz-C_{16} and Lact-Tz-C_{16} was confirmed by X-ray diffraction (XRD). As an example, see the Supporting Information SI5 for Cell-Tz-C_{16}. The lamellar spacing was measured close to 47 Å, which indicates an interdigitated bilayer.

Gel Properties. The solubility and gelation ability of the amphiphilic glycolipids were examined in different solvents by dissolving 5 mg of compound in about 0.1−1 mL of the solvent (i.e., 0.5−5 wt %). The results are summarized in Table 2.

Table 2. Solubility and Gelation Properties of Glycolipids in Different Solvents, after Heating and Cooling to RT[a]

solvent	Cell-Tz-C_{16}	Lact-Tz-C_{16}	Malt-Tz-C_{16}
hexane	I	I	I
ethyl acetate	I	I	I
tetrahydrofuran	I	I	S
dichloromethane	I	I	I
acetone	I	I	I
methanol	P	P	S
water	G[b]	G[c]	G[c]
dimethylsulfoxide	S	S	S

[a]I = insoluble, P = precipitate, S = solution, G = gel. Results for Malt-Tz-C_{16} included as a reference and data taken from ref 18. [b]Gels are formed at 0.5 wt %. [c]Gels are formed at 1 wt %.

Glycoamphiphiles are not soluble at room temperature (RT) in the selected solvents except for DMSO. However, in some of the selected solvents, the glycolipids eventually dissolved on heating. The solution was then cooled to RT, and a solution, a precipitate, or a gel was observed depending on the solvent.

Malt-Tz-C_{16} was studied previously, and it forms a gel in water at a minimum concentration of 1 wt % in the absence of other organic solvents.[18] Changes in the sugar polar head to cellobiose and lactose gives compounds Cell-Tz-C_{16} and Lact-Tz-C_{16}, and these also form gels in water (Figure 4). Maltose and lactose derivatives both gel at a minimum concentration of 1 wt %, while the cellobiose derivative gels at a minimum concentration of 0.5 wt %. To solubilize the glycolipids in

Figure 4. Hydrogel of Cell-Tz-C_{16} (0.5 wt %) and Lact-Tz-C_{16} (1 wt %).

dx.doi.org/10.1021/cm301509v | Chem. Mater. XXXX, XXX, XXX−XXX

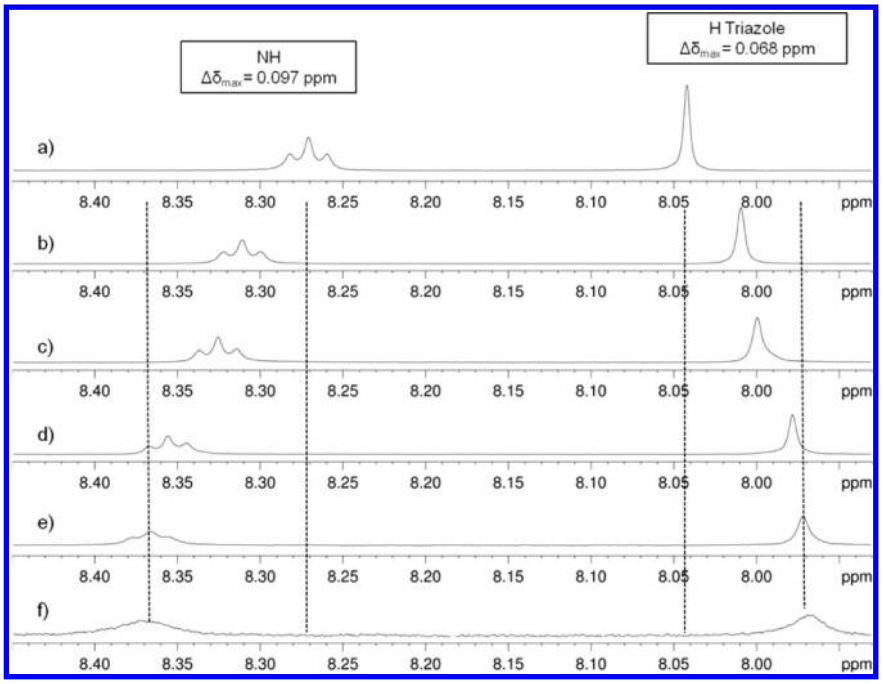

Figure 5. ^{1}H NMR spectra in DMSO-d_6 at 25 °C upon addition of water, (a) 3.4 mg of Lact-Tz-C_{16} in 0.40 mL DMSO-d_6, (b) addition of 0.04 mL H_2O, (c) addition of 0.08 mL H_2O, (d) addition of 0.12 mL H_2O, (e) addition of 0.16 mL H_2O, (f) addition of 0.18 mL H_2O.

water, solutions have to be heated to 90−100 °C and the hydrogel is obtained by cooling. In all cases, the gels are thermoreversible and stable at RT. The sol state can be achieved again by reheating. Thus, the septum-capped test tube was heated in a heating block and the gel−sol transition occurs for Cell-Tz-C_{16} at 95 °C and for Lact-Tz-C_{16} at 85 °C.

To better establish the exact temperature of gel−sol transitions, hydrogels were studied by DSC (under a nitrogen atmosphere, 10 °C min^{-1}). A hydrogel of Cell-Tz-C_{16} (0.5 wt %) shows a broad endothermic peak at around 90 °C (see the Supporting Information, SI6), which is consistent with the results obtained on heating the samples in a heating block and corresponds to the gel−sol transition. A thermal peak was not observed in the cooling scan, however, and in the second and third heating scans, the peak at around 90 °C was again observed, thus confirming the reversibility of this transition. In the case of Lact-Tz-C_{16}, peaks corresponding to the sol−gel transition were not detected by DSC (under the same conditions). In the case of Malt-Tz-C_{16}, it was reported that the gel−sol transition occurs by DSC at around 65 °C.[18] NMR experiments also provide information about gel−sol transitions. On progressive heating of a gel sample in D_2O, the spectrum was fully resolved once the corresponding sol (clear solution) is obtained. For Cell-Tz-C_{16} (0.5 wt % D_2O) was fully resolved at around 95 °C and for Lact-Tz-C_{16} (1 wt % D_2O) was fully resolved at around 80 °C (see the Supporting Information, SI7 and SI8, respectively). Consequently, Cell-Tz-C_{16} and Lact-Tz-C_{16} present a gel state with a higher temperature range. As one would expect, the nature of the sugar polar head, and especially the nature of the glycosidic linkage between the two units (α 1→4 for maltose, β 1→4 for cellobiose and lactose), influences the stability of the supramolecular network that supports the gels, a conclusion based on the differences in the gel−sol temperature as well as differences in the gel concentration.

Two of the driving forces that can promote gel formation are $\pi-\pi$ stacking of aromatic rings and H-bonding. The structure of the synthesized glycoamphiphiles contains a 1,2,3-triazole ring and an amide group, both of which could be responsible for the molecular aggregation and formation of the supramolecular gel. In an effort to confirm the participation of these groups in the supramolecular assembly, the variation of the chemical shift ($\Delta\delta$) was studied in NMR experiments by adding water to a DMSO solution of the glycolipids. A singlet corresponding to the H of the triazole ring is located at 8.04 ppm, and the signal corresponding to the NH group is located at around 8.27 ppm for both compounds in DMSO-d_6, as can be seen in Figure 5 for Lact-Tz-C_{16} (the analogous ^{1}H NMR region for Cell-Tz-C_{16} can be found in the Supporting Information, SI9). The addition of water to the sample led to shielding of the signal due to the H of the triazole ring, a change that indicates the contribution of $\pi-\pi$ stacking to the aggregation.[24] Moreover, a simultaneous deshielding of the NH signal was also observed, and this can be assigned to self-assembly through hydrogen bonding.[24b] The $\Delta\delta_{max}$ value for the H of the triazole is 0.068 ppm, and $\Delta\delta_{max}$ for NH is 0.097 ppm on a sample of 3.4 mg of Lact-Tz-C_{16} in 0.40 mL DMSO-d_6 when 0.16 mL of water (40%) was added. The signals did not shift anymore, and a gel-like structure, suspended in the solvent, is formed when additional water was added in both cases.

The influence of amide groups in the design of hydrogelators is well-known, but the presence of the triazole as the linking unit of the hydrophobic and hydrophilic parts of the synthesized glycoamphiphiles also seem to play an important role. Indeed, the triazole ring is a rigid fragment of the amphiphile structure that can promote the formation of aggregates. Furthermore, its dipole moment also increases the hydrophilicity, thus ensuring appropriate solubility in water, which in turn facilitates the preparation of hydrogels.

Microscopic Gel Characterization. The self-assembled microstructures of the xerogels derived from Cell-Tz-C_{16} and Lact-Tz-C_{16} were studied by SEM and TEM. Additional experiments were performed by ESEM and cryo-TEM in order to better understand the swollen structure in water. AFM

dx.doi.org/10.1021/cm301509v | Chem. Mater. XXXX, XXX, XXX−XXX

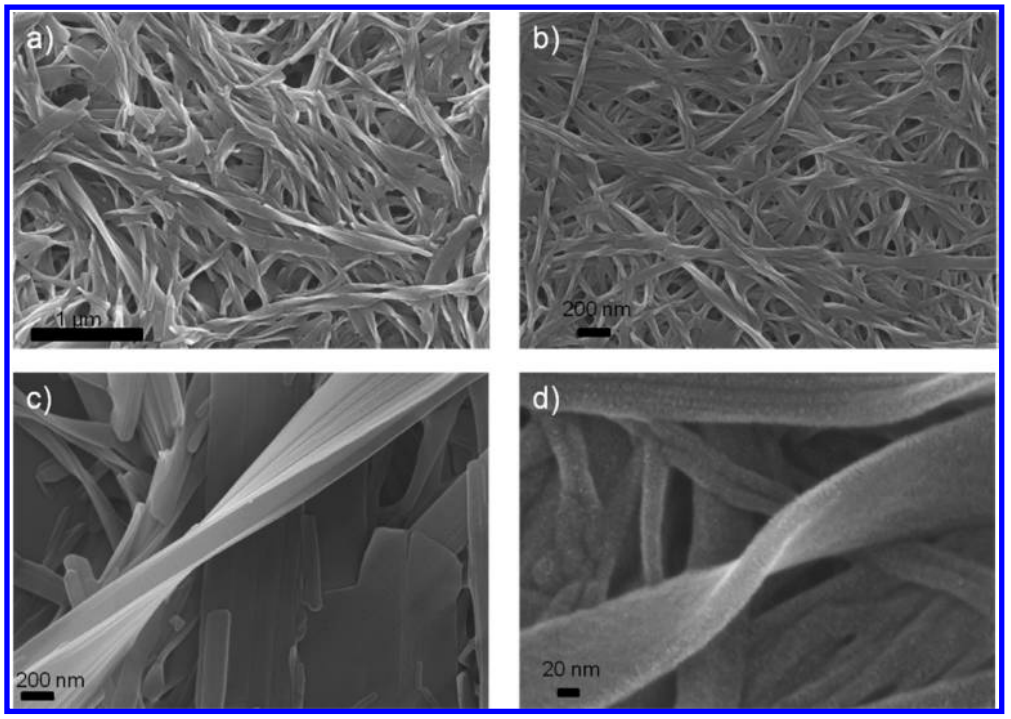

Figure 6. (a) FESEM image of Cell-Tz-C_{16} (0.5 wt % water) xerogel, (b) FESEM image of Lact-Tz-C_{16} (1 wt % water) xerogel, (c) FESEM image of a single ribbon of Cell-Tz-C_{16} (0.5 wt % water) xerogel. (d) FESEM image of a single ribbon of Lact-Tz-C_{16} (1 wt % water) xerogel. The samples were coated with platinum.

measurements were also performed in order to obtain topological information on the structure.

Field emission scanning electron microscopy (FESEM) measurements on the xerogel obtained from Cell-Tz-C_{16} (0.5 wt % gel in water) show a supramolecular fibrillar network formed by bundles of ribbons with a width ranging from around 50 to 400 nm, and a length of several micrometers (Figure 6a). Similar ribbons are also observed for Lact-Tz-C_{16} (1.0 wt % gel in water), with a width ranging around 40 to 150 nm and a length of several μm (Figure 6b). This physical network of ribbons is responsible for the immobilization of water in hydrogels.

When single ribbons are observed, torsion can be detected in the structure. Cell-Tz-C_{16} ribbons exhibit a right-handed twist, as can be seen in Figure 6c, while the torsion in Lact-Tz-C_{16} ribbons leads to a left-handed twist (Figure 6d).

For TEM measurements, gel samples were first diluted down to 0.05 or 0.1 wt % and negatively stained with uranyl acetate. Microphotographs of the physical network and a close up of the ribbon are shown in Figure 7. Upon dilution, TEM micrographs also display a physical network of twisted ribbons that have a width of around 60 to 150 nm for Cell-Tz-C_{16} (see Figure 7a). In Lact-Tz-C_{16}, the ribbons seem to have a more regular width of around 40 nm (see Figure 7b). On careful observation of a single ribbon of Cell-Tz-C_{16} (see Figure 7c), a right-handed twist is detected. In the single ribbon of Lact-Tz-C_{16} (see Figure 7d), a left-handed twist can be observed. The space between two torsions (pitch) seems to be approximately regular within a single ribbon but differs from one fiber to another, especially as the width changes.

ESEM and Cryo-TEM experiments were also carried out in order to better understand the structure without drying the gel. ESEM measurements on the gels provide an insight into the micrometer structure under wet environmental conditions. In the case of Cell-Tz-C_{16}, flat ribbons are observed while Lact-Tz-C_{16} shows a rough brain-like structure (Figure 8). Smaller fibers are detected as the gels are progressively dried. This technique also allows holes in the structure to be viewed (these are easily observed in Cell-Tz-C_{16} in comparison with Lact-Tz-C_{16}, see Figures 8b and d). Significant changes were not observed on studying the same field of view in the samples while progressively decreasing the humidity. This fact shows that the supramolecular 3D network remains very similar when water is removed (see the Supporting Information, SI10).

Cryo-TEM experiments were carried out directly on hydrogels vitrified in liquid ethane. The ribbons resulting from the self-assembly of the amphiphiles were also detected by this technique in both samples. A cryo-TEM microphotograph of the Cell-Tz-C_{16} gel is shown in Figure 9 (for Lact-Tz-C_{16} cryo-TEM results, see the Supporting Information, SI11). On studying the twisted part of the ribbon, it can be seen that the cross sections of the ribbon show alternate dark and bright regions (as can be seen in the zoom of Figure 9) with a thickness of these regions of about 2 and 2.5 nm, respectively. The model shown in Figure 9 is proposed to explain the assembly of amphiphiles into ribbons and the resulting layered structure of the cross-section. This layered structure of the cross-section of ribbons is formed by alternating hydrophilic parts, consisting of a bilayer of sugar polar heads, and hydrophobic parts of interdigitated aliphatic domains. In fact, the theoretical length of the hydrophobic part is about 25 Å (18.5 Å for the palmitic chain and 6.6 Å for amide and triazole ring), which is in accordance with the thickness of the bright motives of around 2.5 nm. In the same way the theoretical length of the disaccharide is around 10 Å. The thickness of the dark motive is around 2 nm, which is in accordance with a disaccharide bilayer.

dx.doi.org/10.1021/cm301509v | *Chem. Mater.* XXXX, XXX, XXX−XXX

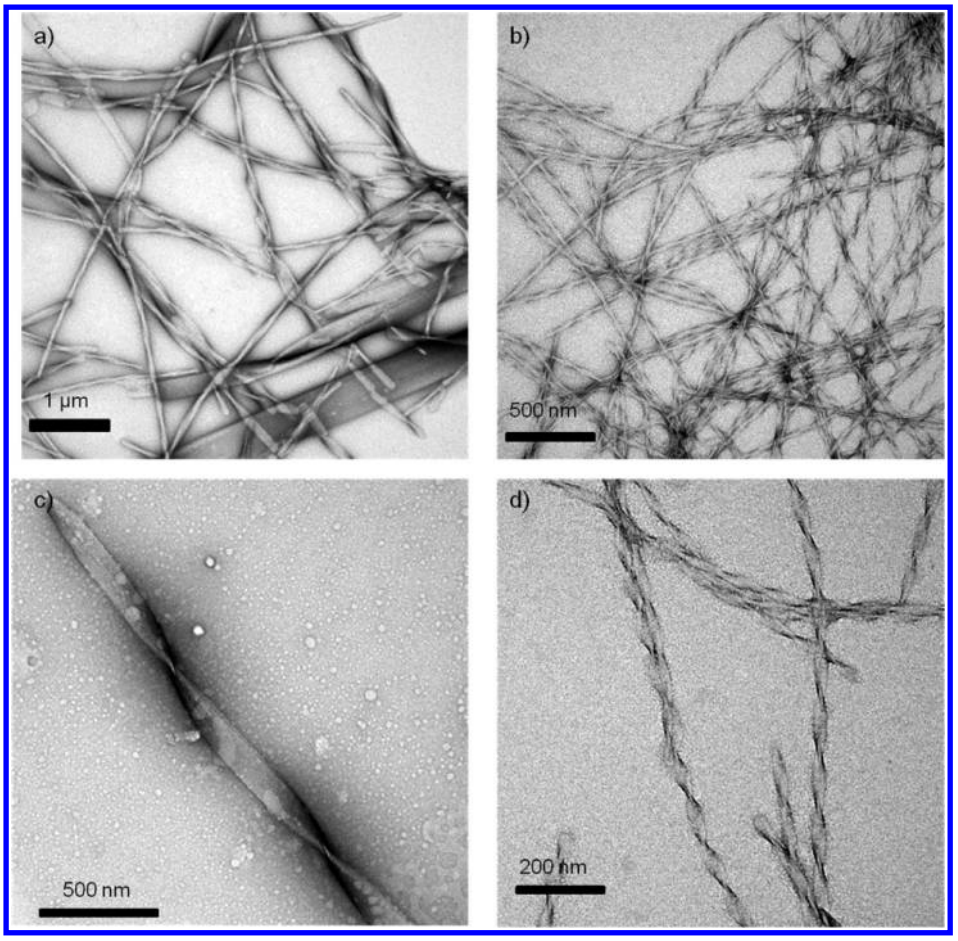

Figure 7. (a) TEM image of Cell-Tz-C_{16} (0.05 wt %), (b) TEM image of Lact-Tz-C_{16} (0.1 wt % water), (c) TEM image of a single ribbon of Cell-Tz-C_{16} (0.05 wt % water) with a right handed twist, (d) TEM image of a single ribbon of Lact-Tz-C_{16} (0.1 wt % water) with a left handed twist. TEM images were taken on samples that were dried and negatively stained with uranyl acetate (1 wt % water).

AFM measurements were performed on a drop of the gel placed onto graphite and subsequently dried with air. It can be observed in Figure 10 that the samples have opposite twisted ribbons in hydrogels from Cell-Tz-C_{16} and Lact-Tz-C_{16}—a situation in accordance with the results obtained by electron microscopy. As an example, for a single ribbon of Cell-Tz-C_{16}, the profiles of two different zones are represented in Figure 10d. The widths for the two profiles are around 125 nm. A height of 42 nm was determined at the highest point (profile 1, black) and 26 nm at the torsion (profile 2, red).

Circular Dichroism Measurements. The twisted ribbons detected in gels are a consequence of a chiral supramolecular arrangement of self-assembled amphiphiles. The opposite handedness of the ribbons, as observed by the different microscopic techniques, seems to be consequence of an opposite supramolecular chirality. In an attempt to confirm this opposite supramolecular chirality, circular dichroism (CD) measurements were carried out on the gels and the results are represented in Figure 11.

The λ_{max} value for a hydrogel of Cell-Tz-C_{16} at minimum gelator concentration (0.5 wt %) in the UV absorption spectrum appears at around 230 nm and this absorption can be assigned to the triazole group. The hydrogel of this compound (0.5 wt %), when placed between two quartz discs, exhibited a positive Cotton effect, for which the θ_{max} value appeared to be slightly displaced from the λ_{max} in the UV spectrum to 240 nm (please see the Supporting Information, SI12, for similar figure at concentration of Cell-Tz-C_{16} gel at 1 wt %). For the hydrogel derived from Lact-Tz-C_{16} at minimum gelator concentration (1 wt %), the λ_{max} (due to the triazole group) appears at 227 nm, but in this case, the Cotton effect was negative. The θ_{min} value appeared to be displaced from the λ_{max} in the UV spectrum to 237 nm. For this compound, the values and signal of the Cotton effect matched those obtained for an aqueous gel of Malt-Tz-C_{16} at 1 wt %. It was confirmed that the contribution of the linear dichroism (LD) to the CD spectrum is negligible by comparing several CD spectra recorded at different angles around the incident light beam.

The opposite CD signals can be attributed to an opposite chiral supramolecular arrangement of the molecules, a structure that is the origin of the opposite handeness observed in the ribbons. This fact shows that the stereochemical arrangement of only one hydroxyl group (equatorial OH-4 in Cell-Tz-C_{16} vs axial OH-4 in Lact-Tz-C_{16}), or the arrangement of the glycosidic bond (β 1→4 in Cell-Tz-C_{16} vs α 1→4 in Malt-Tz-C_{16}), has a significant effect on the preferential conformation[21] and the self-assembly and supramolecular organization[22] of these molecules.

■ CONCLUSIONS

New amphiphiles based on disaccharides as polar head groups have been synthesized, and their liquid crystalline and gel-forming properties have been investigated. Glycolipids were prepared by a copper(I)-catalyzed azide−alkyne [3 + 2]

dx.doi.org/10.1021/cm301509v | *Chem. Mater.* XXXX, XXX, XXX−XXX

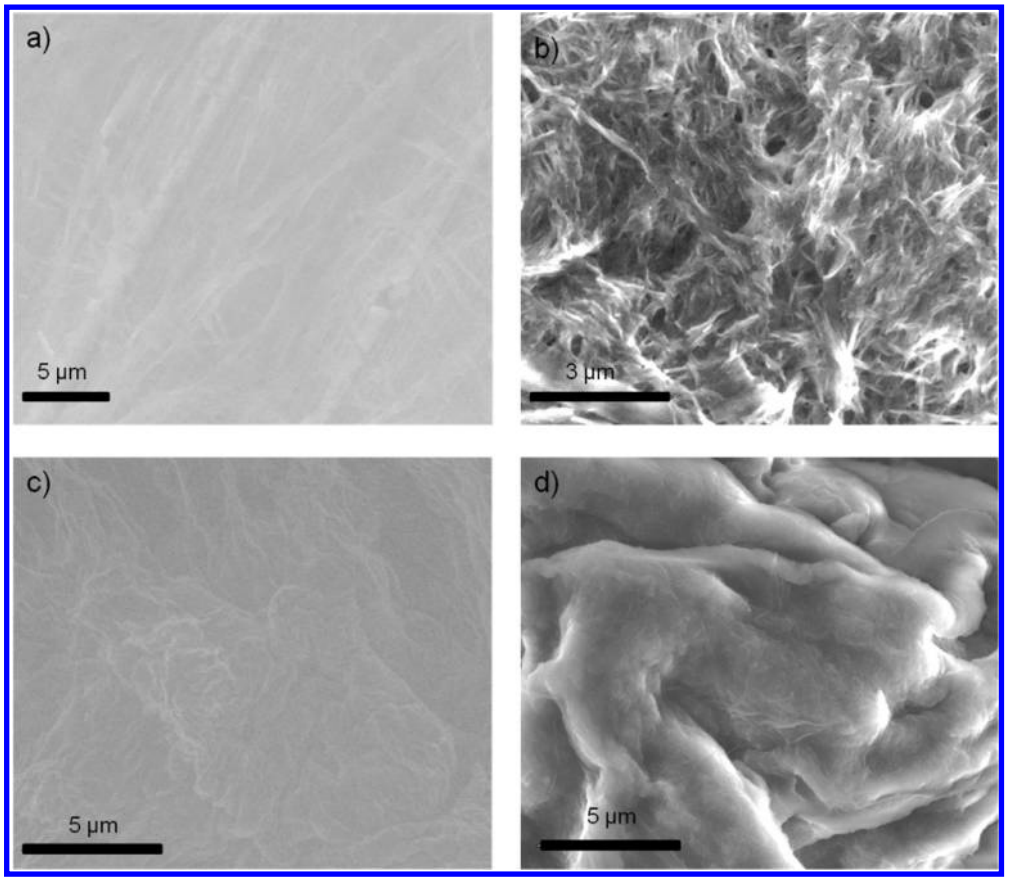

Figure 8. (a) ESEM image of Cell-Tz-C_{16} (0.5 wt % water) 99.9% humidity, 3.0 °C, 759 Pa, (b) ESEM image of Cell-Tz-C_{16} (0.5 wt % water) 20% humidity, 3.0 °C, 152 Pa, (c) ESEM image of Lact-Tz-C_{16} (1 wt % water) 99.9% humidity, 3.0 °C, 759 Pa, (d) ESEM image of Lact-Tz-C_{16} (1 wt % water) 20.0% humidity, 3.0 °C, 152 Pa.

cycloaddition to link a cellobiose or lactose to a palmitoyl derivative bearing an alkyne group.

The compounds synthesized exhibit a mesomorphic lamellar fluid state and are able to gel in pure water. These hydrogels are stable at room temperature, and the gel−sol transition is thermoreversible. The minimum concentrations to form a gel are 1 or 0.5 wt % for lactose or cellobiose compounds, respectively. The resulting self-assembled fibrillar network was studied by different microscopic techniques, either in the xerogel state by TEM, FESEM, and AFM or in a wet environment by cryo-TEM and ESEM. Twisted ribbons were observed, and the supramolecular chirality was supported by the observation of a CD effect. The opposite direction of the torsion and sense of the CD signal were found to depend on the sugar polar head. This study has led to a deeper insight into the supramolecular organization of hydrogels based on low molecular weight sugar amphiphiles.

EXPERIMENTAL SECTION

D-lactose monohydrate and cellobiose octaacetate were purchased from Aldrich and were used without previous purification. Lactose octaacetate[25] (**1**) and N-propargyl palmitoylamide (**4**)[18] were synthesized according to a previously described procedure.

Octa-O-acetyl-β-lactose $C_{28}H_{38}O_{19}$ (1). ^{1}H NMR (500 MHz, $CDCl_3$, 25 °C, δ ppm): (**1β**) 1.96 (s, 3H), 2.02 (s, 3H), 2.03 (s, 3H), 2.04 (s, 3H) 2.06 (s, 3H), 2.09 (s, 3H), 2.11 (s, 3H), 2,15 (s, 3H) CH_3—CO—O— ×8, 3.75 (ddd, 1H, $J_{5',6'b}$ = 2.0 Hz, $J_{5',6'a}$ = 4.8 Hz, $J_{4',5'}$ = 9.8 Hz, $H5'_\beta$), 3.81 − 3.88 (m, 2H, $H5_\beta$, $H4'_\beta$), 4.04−4.16 (m, 3H, $H6a_\beta$, $H6b_\beta$, $H6'a_\beta$), 4.41−4.49 (m, 2H, $H6'b_\beta$, $H1_\beta$), 4.94 (dd, 1H, $J_{3,4}$ = 3.4 Hz, $J_{2,3}$ = 10.5 Hz, $H3_\beta$), 5.04 (dd, 1H, $J_{1',2'}$ = 8.2 Hz, $J_{2',3'}$ = 8.7 Hz, $H2'_\beta$), 5.10 (dd, 1H, $J_{1,2}$ = 7.8 Hz, $J_{2,3}$ = 10.5 Hz, $H2_\beta$), 5.23 (dd, 1H, $J_{2',3'}$ = 8.7 Hz, $J_{3',4'}$ = 9.3 Hz, $H3'_\beta$), 5.34 (dd, 1H, $J_{3,4}$ = 3.4 Hz, $J_{4,5}$ = 1.1 Hz, $H4_\beta$), 5.66 (d, 1H, $J_{1',2'}$ = 8.2 Hz, $H1'_\beta$). (**1α**) 1.96 (s, 3H), 2.00 (s, 3H), 2.05 (s, 3H), 2.05 (s, 3H) 2.06 (s, 3H), 2.12 (s, 3H), 2.15 (s, 3H), 2,17 (s, 3H) CH_3—CO—O— ×8, 3,78−3.90 (m, 2H, $H4'_\alpha$, $H5_\alpha$), 3.97 (m, 1H, $H5'_\alpha$), 4.05−4.18 (m, 2H, $H6a_\alpha$, $H6b_\alpha$), 4.12−4.18 (m, 1H, $H6'a_\alpha$), 4.43−4.51 (m, 2H, $H6'b_\alpha$, $H1_\alpha$), 4.94−4.97 (m, 1H, $H3_\alpha$), 5.00 (dd, 1H, $J_{1',2'}$ = 3.7 Hz, $J_{2',3'}$ = 10.5 Hz, $H2'_\alpha$), 5.10−5.14 (m, 1H, $H2\alpha$), 5.34−5.37 (m, 1H, $H4\alpha$,), 5.45 (dd, 1H, $J_{2',3'}$ = 10.5 Hz, $J_{3',4'}$ = 9.3 Hz, $H3'_\alpha$), 6.24 (d, 1H, $J_{1',2'}$ = 3.7 Hz, $H1'\alpha$). ^{13}C NMR (125 MHz, $CDCl_3$, 25 °C, δ ppm): (**1β**) 20.7, 20.7, 20.8, 20.9, 20.9, 21.0 CH_3—CO— ×8, 61.0, 61.9 $C6_\beta$, $C6'_\beta$, 66.7 $C4_\beta$, 69.1 $C2_\beta$, 70.6 $C2'_\beta$, 70.9, 71.7, $C5_\beta$, $C3_\beta$, 72.8 $C3'_\beta$, 73.6 $C5'_\beta$, 75.8 $C4'_\beta$, 91.7 $C1'_\beta$, 101.6 $C1_\beta$, 169.0, 169.2 C2—O—*CO*—, C1′—O—*CO*—, 169.7, 169.8 C2′—O—*CO*—, C3′—O—CO—, 170.2, 170.3, 170.5, 170.5 C3—O—CO—, C4—O—CO—, C6—O—CO—, C6′—O—CO. (**1α**) 20.8, 21.1, 20,7, 21,1 CH_3—CO— ×8, 60.9, 61.6, $C6_\alpha$, $C6'_\alpha$ 69.3, 69.8, 71.1, 75.9, $C_{X\alpha}$ 69.5 $C3'_\alpha$, 70.8 $C5'_\alpha$, 89.1 $C1'_\alpha$, 101.3 $C1_\alpha$ 169.1, 169.3, 170.1 CH_3—O—CO—, other C cannot be assigned.

MALDI-TOF MS (DIT+NaTFA): 701.2 $[M + Na]^+$.

IR (KBr, cm^{-1}): 3481, 2983, 1754, 1371, 1219, 1048, 898, 601.

Synthesis of Hepta-O-acetyl-β-lactosyl Azide (2) and Hepta-O-acetyl-β-cellobiosyl Azide (3). Trimethylsilyl azide (1.1 mL, 8.36 mmol) and tin tetrachloride (350 μL, 2.99 mmol) were added, at room temperature and under argon, to a solution of lactose octaacetate (**1**) or cellobiose octaacetate (4.01 g, 5.92 mmol) in dry CH_2Cl_2 (15 mL). The reaction mixture was stirred at room temperature, and the reaction was monitored by TLC (1:1 hexane/ethyl acetate). After 24 h, CH_2Cl_2 was added and the solution was washed with saturated Na_2CO_3 and twice with water. The organic layer was dried over $MgSO_4$, filtered, and evaporated under reduced pressure. The product

dx.doi.org/10.1021/cm301509v | Chem. Mater. XXXX, XXX, XXX−XXX

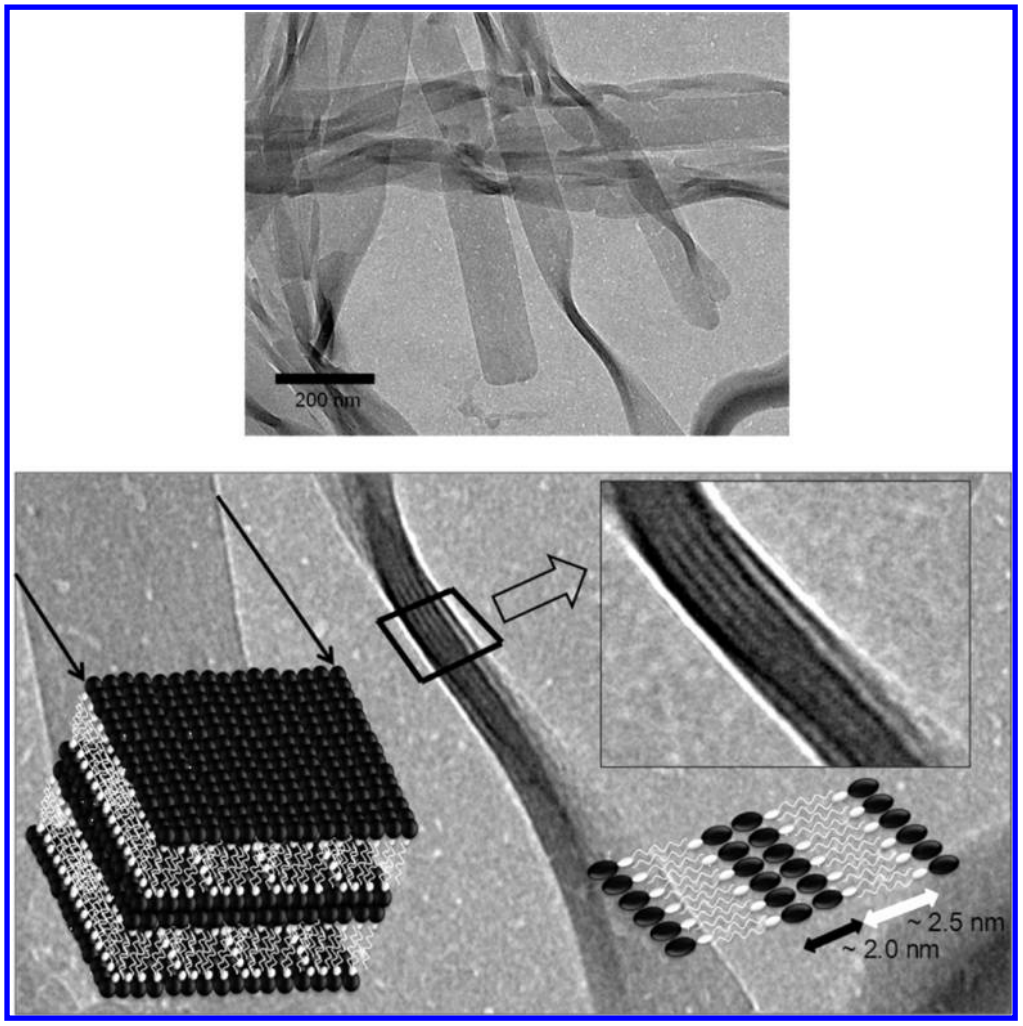

Figure 9. Cryo-TEM image of Cell-Tz-C_{16} 0.5 wt % water gel (top) and model proposed for molecular arrangement (bottom): Ribbons formed by alternating hydrophobic sugar regions and interdigitated hydrophobic regions. A close up of the cross-section of the ribbon is shown on the right corner (see the model for this cross-section).

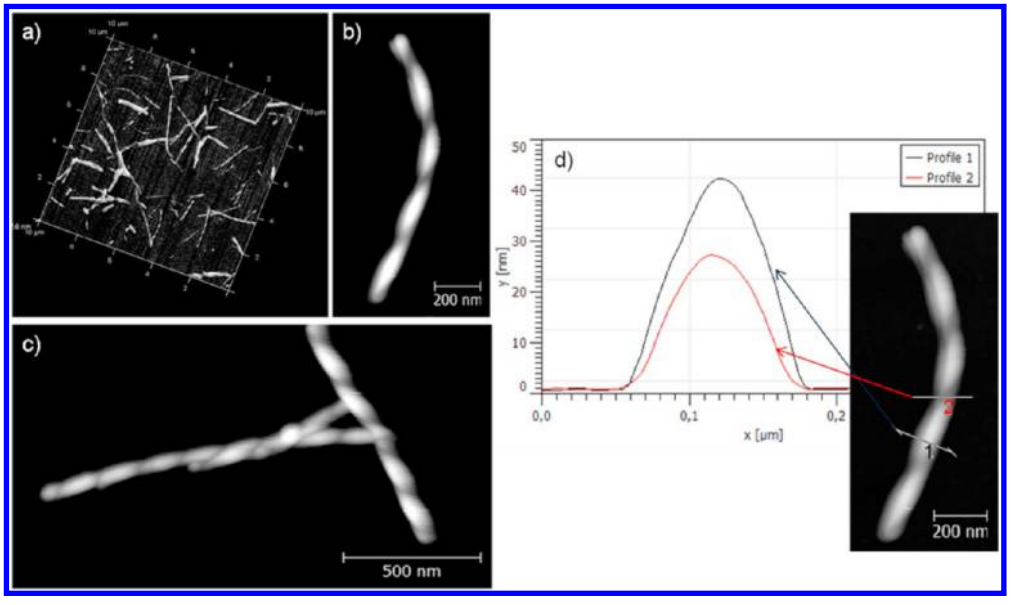

Figure 10. AFM microphotographs of hydrogels (a) Cell-Tz-C_{16} (0.5 wt %), (b) single ribbon of Cell-Tz-C_{16} (0.5 wt %), (c) single ribbons of Lact-Tz-C_{16} (1 wt %), (d) profiles of two different zones of a single ribbon of Cell-Tz-C_{16} (0.5 wt %).

dx.doi.org/10.1021/cm301509v | *Chem. Mater.* XXXX, XXX, XXX−XXX

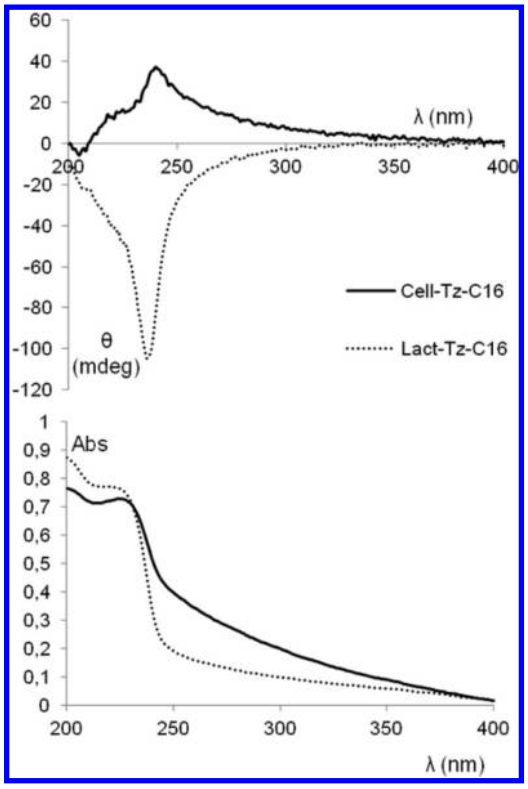

Figure 11. CD (top) and UV−vis (bottom) spectra of hydrogels derived from Cell-Tz-C_{16}, (0.5 wt %), solid line, and Lact-Tz-C_{16} (1 wt %), dashed line.

was purified by flash chromatography using hexane/ethyl acetate 1:1. A white solid was obtained (3.19 g, 82%).

Hepta-O-acetyl-β-lactosyl Azide $C_{26}H_{35}N_3O_{17}$ (2). ^{1}H NMR (400 MHz, $CDCl_3$, 25 °C, δ ppm): 1.96 (s, 3H), 2.04 (s, 3H), 2.04 (s, 3H), 2.06 (s, 3H), 2.06 (s, 3H), 2.13 (s, 3H), 2.14 (s, 3H) CH_3—CO—O— ×7, 3.70 (ddd, 1H, $J_{5',6'b}$ = 5.1 Hz, $J_{5',6'a}$ = 2.2 Hz, $J_{4',5'}$ = 9.9 Hz, *H5′*), 3.81 (dd, 1H, $J_{3',4'}$ = 9.1 Hz, $J_{4',5'}$ = 9.9 Hz, *H4′*), 3.87 (ddd, 1H, $J_{5,6b}$ = 7.3 Hz, $J_{5,6a}$ = 7.3 Hz, $J_{5,4}$ = 0.9 Hz, *H5*), 4.05−4.14 (m, 3H, *H6a, H6b,H6′$_b$*), 4.47−4.52 (m, 2H, *H1, H6′$_a$*), 4.62 (d, 1H, $J_{1',2'}$ = 8.8 Hz, *H1′*, 4.85 (dd, 1H, $J_{1',2'}$ = 8.8 Hz, $J_{2',3'}$ = 9.3 Hz, *H2′*), 4.95 (dd, 1H, $J_{3,4}$ = 3.5 Hz, $J_{2,3}$ = 10.5 Hz, *H3*), 5.10 (dd, 1H, $J_{1,2}$ = 7.9 Hz, $J_{2,3}$ = 10.5 Hz, *H2*), 5.20 (dd,1H, $J_{2',3'}$ = 9.3 Hz, $J_{3',4'}$ = 9.1 Hz, *H3′*), 5.34 (dd, 1H, $J_{3,4}$ = 3.5 Hz, $J_{4,5}$ = 0.9 Hz, *H4*).

^{13}C NMR (100 MHz, $CDCl_3$, 25 °C, δ ppm): 20.6, 20.7, 20.7, 20.7 20.8, 20.9 CH_3—CO— ×7, 60.9 *C6*, 61.8 *C6′*, 66.7 *C4*, 69.2 *C2*, 70.8, 71.0, 71.1 *C3*, *C5*, *C2′*, 72.6 *C3′*, 74.9 *C5′*, 75.9 *C4′*, 87.8 *C1′*, 101.2 *C1*, 169.2 C2—O—CO—, 169.6 C2′—O—CO—, 169.7 C3′—O—CO—, 170.1, 170.2 C3—O—CO—, C4—O—CO—, 170.4, 170.5 C6—O—CO—, C6′—O—CO—.

MALDI-TOF MS (DIT+NaTFA): 684.3 $[M + Na]^+$.

IR (KBr, cm^{-1}): 3481, 2983, 2122, 1753, 1372, 1230, 1057, 899, 602.

Hepta-O-acetyl-β-cellobiosyl Azide $C_{26}H_{35}N_3O_{17}$ (3). ^{1}H NMR (400 MHz, $CDCl_3$, 25 °C, δ ppm): 1.98 (s, 3H), 2.00 (s, 3H), 2.02 (s, 3H), 2.03 (s, 3H), 2.06 (s,3H), 2.08 (s, 3H), 2.14 (s,3H) CH_3—CO—O— ×7, 3.61−3.73 (m, 2H, *H5, H5′*), 3.79 (dd, 1H, $J_{3',4'}$ = 9.0 Hz, $J_{4',5'}$ = 9.9 Hz, *H4′*), 4.03 (dd, 1H, $J_{5,6a}$ = 2.3 Hz, $J_{6a,6b}$ = 12.9 Hz, *H6a*), 4.11 (dd, 1H, $J_{5',6'a}$ = 4.9 Hz, $J_{6'a,6'b}$ = 12.2 Hz, *H6′a*), 4.37 (dd, 1H, $J_{5,6b}$ = 4.5 Hz, $J_{6a,6b}$ = 12.9 Hz, *H6b*), 4.48−4.56 (m, 2H, *H1, H6′$_b$*), 4.61 (d, 1H, $J_{1',2'}$ = 8.9 Hz, *H1′*), 4.86 (dd, 1H, $J_{1',2'}$ = 8.9 Hz, $J_{2',3'}$ = 8.4 Hz, *H2′*), 4.92 (dd, 1H, $J_{1,2}$ = 7.9 Hz, $J_{2,3}$ = 9.1 Hz, *H2*), 5.06 (dd, 1H, $J_{3,4}$ = 9.4 Hz, $J_{4,5}$ = 9.7 Hz, *H4*), 5.14 (dd, 1H, $J_{2,3}$ = 9.1 Hz, $J_{3,4}$ = 9.4 Hz, *H3*), 5.18 (dd,1H, $J_{2',3'}$ = 8.4 Hz, $J_{3',4'}$ = 9.0 Hz, *H3′*).

^{13}C NMR (100 MHz, $CDCl_3$, 25 °C, δ ppm): 20.6, 20.7, 20.7, 20.8, 20.9 CH_3—CO— ×7, 61.6, 61.7 *C6*, *C6′*, 67.8 *C4*, 71.0 *C2′*, 71.7 *C2*, 72.2, 72.3, 73.0, 75.0 *C3*, *C5*, *C3′*, *C5′*, 76.1 *C4′*, 87.8 *C1′*, 100.8 *C1*, 169.2 C2—O—CO—, 169.4 C4—O—CO—, 169.6 *C2′*—O—CO—, 169.8 C3′—O—CO—, 170.3, 170.4, 170.6 C3—O—CO—, C6—O—CO—, C6′—O—CO—.

MALDI-TOF MS (DIT+NaTFA): 684.0 $[M + Na]^+$.

IR (KBr, cm^{-1}): 3474, 2954, 2879, 2121, 1748, 1371, 1238, 1066, 1046, 904, 600.

N-Propargylpalmitoylamide $C_{19}H_{35}NO$ (4). ^{1}H NMR (300 MHz, $CDCl_3$, 25 °C, δ ppm): 0.87 (t, 3H, *J* = 6,5 Hz, —CH_2—CH_3), 1.20−1.40 (m, 24H, —CH_2—$(CH_2)_{12}$—), 1.59−1.64 (m, 2H, —CH_2—$(CH_2)_{12}$—), 2.18 (t, 2H, *J* = 7,5 Hz, —CO—CH_2—), 2.22 (t, 1H, *J* = 2,4 Hz, HC≡C—), 4.05 (dd, 2H, $J_{CH2,C\equiv CH}$ = 2,5 Hz, $J_{CH2,NH}$ = 5,0 Hz, ≡C—CH_2—NH—), 5.63 (s, 1H, N*H*).

^{13}C NMR (75 MHz, $CDCl_3$, 25 °C, δ ppm): 14.1 —CH_2—CH_3, 25.6 —CH_2—$(CH_2)_{12}$, 22.7, 29.2, 29.3, 29.3, 29.4, 29.5, 29.6, 29.7, 29.7, 31.9 —$(CH_2)_{12}$—, ≡C—CH_2—NH, 36.5 —CO—CH_2—$(CH_2)_{13}$, 71.5 HC≡C, 79.7 HC≡C—CH_2, 172.7 NH—CO—CH_2.

Micro-TOF MS: 294.2773 $[M+H]^+$ calcd 293.2713; 316.2612 $[M+Na]^+$, calcd 316.2611.

IR (KBr, cm^{-1}): 3292, 3073, 2955, 2918, 2848, 1639, 1553, 1472, 1462, 1275, 729, 719, 689, 666, 631, 570.

Synthesis of Acetylated Glycolipids OAc-Lact-Tz- C_{16} and OAc- Cell-Tz-C_{16}. Propargyl derivative **4** (0.44 g, 1.50 mmol), azide derivative **2** or **3** (1.00 g, 1.51 mmol), copper(I) bromide (46.6 mg, 0.32 mol), and N-pentamethyldiethylenetriamine (PMDETA) (65 μL, 0.31 mmol) were dissolved in anhydrous dimethylformamide (10 mL) under argon atmosphere. The mixture was stirred at room temperature for 2 days. The reaction was monitored by TLC with hexane/ethyl acetate 1:1 as eluent. The catalyst was then removed by filtration, and the solvent was removed under reduced pressure. The reaction was poured into 150 mL of water. The aqueous phase was extracted three times, each with 200 mL of hexane/ethyl acetate 1:1. The organic phase was dried with anhydrous $MgSO_4$. The solution was filtered, and the solvent was removed under reduced pressure. The resulting white solid was purified by flash chromatography using initially dichloromethane/ethyl acetate 1:1 and then increasing the polarity. A white solid was obtained (1.17 g, 81% of OAc-Lact-Tz-C_{16}) (1.14 g, 80% of OAc-Cell-Tz-C_{16}).

OAc-Lact-Tz-C_{16} $C_{45}H_{70}N_4O_{18}$. ^{1}H NMR (400 MHz, $CDCl_3$, 25 °C, δ ppm): 0.87 (t, 3H, *J* = 6.8 Hz, —$(CH_{2)12}$—CH_3), 1.20−1.36 (m, 24H, —$(CH_2)_{12}$—), 1.56−1.65 (m, 2H, CO—CH_2—CH_2—$(CH_2)_{12}$), 1.86 (s, 3H), 1.97 (s, 3H), 2.05 (s, 3H), 2.06 (s, 3H), 2.08 (s, 3H), 2.11(s, 3H), 2.16 (s, 3H) CH_3—CO—O ×7, 2.18 (t, 2H, *J* = 7.3 Hz, CO—CH_2—CH_2), 3.85−3.99 (m, 3H, *H4′,H5, H5′*), 4.05−4.19 (m, 3H, *H6a, H6$_b$, H6′$_a$*), 4.42−4.57 (m, 4H, C—CH_2—NH, *H1, H6′$_b$*), 4.97 (dd, 1H, $J_{2,3}$ = 10.4 Hz, $J_{3,4}$ = 3.5 Hz, *H3*), 5.12 (dd, 1H, $J_{1,2}$ = 7.9 Hz, $J_{2,3}$ = 10.4 Hz, *H2*), 5.33−5.44 (m, 3H, *H2′*, *H3′*, *H4*), 5.78 (d, 1H, $J_{1',2'}$ = 9.2 Hz, *H1′*), 6.11 (t, 1H, *J* = 5.3 Hz, —CH_2—N*H*—CO), 7.71 (s, 1H, N—C*H*=C—CH_2 triazole).

^{13}C NMR (100 MHz, $CDCl_3$, 25 °C, δ ppm): 14.2 —$(CH_2)_{12}$—CH_3, 20.3, 20.6, 20.7, 20.8, 20.9 CH_3—CO—O ×7, 22.8 CH_2—CH_2—$CH_2)_{12}$—, 25.7 CO—CH_2—CH_2—$(CH_2)_{12}$, 29.4, 29.5, 29.5, 29.6, 29.7, 29.8, 29.8, 32.1, —$(CH_2)_{12}$—, 34.9 C—CH_2—NH, 36.7 CO—CH_2—CH_2, 60.9, 61.8 *C6, C6′*, 66.7 C4, 69.1 C2, 70.7, 70.9, 71.0, 72.5, 75.5, 75.9, *C2′*, *C3′*, *C4′*, *C5′*, *C3*, *C5*, 85.6 *C1′*, 101.2 *C1*, 120.8 *CH* triazole, 145.5 *C* triazole, 169.2, 169.2, 169.6, 170.2, 170.2, 170.3, 170.5 CH_3—CO—O—, 173.4 NH—CO—CH_2.

MALDI-TOF MS (DIT+NaTFA): 977.4 $[M + Na]^+$.

Anal. calcd for $C_{45}H_{70}N_4O_{18}$: C, 56.59; H, 7.39; N, 5.87. Found: C, 56.88; H, 7.73; N, 5.84.

IR (KBr, cm^{-1}): 3398, 2925, 2854, 1754, 1658, 1371, 1230, 1047, 919, 603.

OAc-Cell-Tz-C_{16} $C_{45}H_{70}N_4O_{18}$. ^{1}H NMR (400 MHz, $CDCl_3$, 25 °C, δ ppm): 0.87 (t, 3H, *J* = 6.8 Hz, —$(CH_2)_{12}$—CH_3), 1.19−1.35 (m, 24H, —$(CH_2)_{12}$—), 1.55−1.65 (m, 2H, CO—CH_2—CH_2—$(CH_2)_{12}$), 1.86 (s, 3H), 1.98 (s, 3H), 2.01 (s, 3H), 2.03 (s, 3H), 2.04 (s, 3H), 2.10 (s, 3H), 2.11 (s, 3H) CH_3—CO—O ×7, 2.17 (t, 2H, *J* = 7.3 Hz, CO—CH_2—CH_2), 3.69 (ddd, 1H, $J_{4,5}$ = 9.6 Hz, $J_{5,6a}$ = 2.1 Hz, $J_{5,6b}$ = 4.3 Hz,, *H5*), 3.84−3.98 (m, 2H, *H4′*, *H5′*), 4.06 (dd, 1H, $J_{5,6a}$ = 2.1 Hz, $J_{6a,6b}$ = 12.5 Hz, *H6a*), 4.12 (dd, 1H, $J_{5',6'a}$ = 4.7

dx.doi.org/10.1021/cm301509v | *Chem. Mater.* XXXX, XXX, XXX−XXX

Hz, $J_{6'a,6'b}$ = 12.2 Hz, *H6′a*), 4.38 (dd, 1H, $J_{5,6b}$ = 4.3 Hz, $J_{6a,6b}$ = 12.5 Hz, *H6b*), 4.43−4.53 (m, 3H, *H6′b*, C≡C—CH_2—NH), 4.55 (d, 1H, $J_{1,2}$ = 8.2 Hz, *H1*), 4.94 (dd, 1H, $J_{1,2}$ = 8.2 Hz, $J_{2,3}$ = 9.4 Hz, *H2*), 5.07 (dd, 1H, $J_{3,4}$ = 9.5 Hz, $J_{4,5}$ = 9.6 Hz, *H4*), 5.16 (dd, 1H, $J_{2,3}$ = 9.4 Hz, $J_{3,4}$ = 9.5 Hz, *H3*), 5.33−5.42 (m, 2H, *H2′*, *H3′*), 5.73−5.73−5.81 (m, 1H, *H1′*), 6.11 (t, 1H, *J* = 5.6 Hz, —CH_2—N*H*—CO), 7.70 (s, 1H, N—C*H*=C—CH_2 triazole).

^{13}C NMR (100 MHz, $CDCl_3$, 25 °C, δ ppm): 14.4 —(CH_2)$_{12}$—*C*H_3, 20.5, 20.7, 20.8, 21.0, 21.1 *C*H_3—CO—O ×7, 23.0 —(*C*H_2)$_{12}$—, 25.8 CO—CH_2—*C*H_2—(*C*H_2)$_{12}$, 29.6, 29.6, 29.7, 29.8, 29.9, 29.9, 30.0, 32.2, —(*C*H_2)$_{12}$—, 35.1 C—CH_2—NH, 36.9 CO—*C*H_2—CH_2, 61.9 ×2 *C6, C6′*, 68.0 *C4*, 70.8 *C2′*or *C3′*, 71.9 *C2*, 72.5, 72.6 *C5, C2′*or *C3′*, 73.2 *C3*, 76.0 *C4′*, 76.3 *C5′*, 85.9 *C1′*, 100,1 *C1*, 121.2 *C*H triazole, 145.7 *C* triazole, 169.3 C2′—O—*C*O— or C3′—O—*C*O—, 169.4 C2—O—*C*O—, 169.6 C4—O—*C*O—, 169.8 C2′—O—*C*O— or C3′—O—*C*O—, 170.4, 170.5 C3—O—*C*O, C6′—O—*C*O, 170.8 C6—O—*C*O, 173.6 NH—*C*O—CH$_2$.

MALDI-TOF MS (DIT+NaTFA): 977.4 [M + Na]$^+$.

Anal. calcd for $C_{45}H_{70}N_4O_{18}$: C, 56.59; H, 7.39; N, 5.87. Found: C, 57.00; H, 7.75; N, 5.93.

IR (KBr, cm^{-1}): 3360, 3073, 2923, 2852, 1750, 1650, 1377, 1228, 1044, 906, 599.

Synthesis of Glycolipids Lact-Tz-C_{16} and Cell-Tz-C_{16}. The protected triazole-disaccharide-heptaacetate derivatives (OAc-Lact-Tz-C_{16} and OAc-Cell-Tz-C_{16}) (401 mg, 0.42 mmol) were dissolved in 25 mL of anhydrous methanol. Sodium methoxide (160 mg, 2.96 mmol) was added. The solution was stirred at room temperature until the reaction was complete (TLC, dichoromethane/ethyl acetate 1:1). Amberlyst IR 120 (H^+ form) was added to exchange sodium ions; the resin was filtered off. A white solid was obtained (220 mg, 80% for Lact-Tz-C_{16}) (214 mg, 77% for Cell-Tz-C_{16}).

Lact-Tz-C_{16} $C_{31}H_{56}N_4O_{11}$. ^{1}H NMR (400 MHz, MeOD, 50 °C, δ ppm): 0.90 (t, 3H, *J* = 6.9 Hz, —(CH_2)$_{12}$—*C*H_3), 1.22−1.40 (m, 24H, —(*C*H_2)$_{12}$—), 1.56−1.66 (m, 2H, CO−CH_2—*C*H_2—(CH_2)$_{12}$), 2.21 (t, 2H, *J* = 7.3 Hz, CO—*C*H_2—CH_2), 3.50 (dd, 1H, $J_{2,3}$ = 9.7 Hz, $J_{3,4}$ = 3.3 Hz, *H3*), 3.59 (dd, 1H, $J_{1,2}$ = 7.8 Hz, $J_{2,3}$ = 9.7 Hz, *H2*), 3.82−3.86 (m, 1H, *H4*), 3.60−3.64 (m, 1H), 3.69−3.82 (m, 5H), 3.87−3.91 (m, 2H, *H3′*,*H4′*, *HS′*, *H6′$_a$*, *H6′$_b$*, *HS*, *H6$_a$*, *H6$_b$*), 3.95 (dd, 1H, $J_{1',2'}$ = 9.2 Hz, $J_{2',3'}$ = 8.9 Hz, *H2′*), 4.42 (d, 1H, $J_{1,2}$ = 7.8 Hz, *H1*), 4.44 (s, 1H, —CH_2—NH—CO), 5.60 (d, 1H, $J_{1'-2'}$ = 9.2 Hz, *H1′*), 8.02 (s, 1H, C*H* triazole).

^{13}C NMR (100 MHz, MeOD, 50 °C, δ ppm): 14.3 —(CH_2)$_{12}$—*C*H_3, 23.6 —(CH_2)$_{12}$—, 26.8 CO—CH_2—CH_2—(CH_2)$_{12}$—, 30.3, 30.3, 30.5, 30.6, 30.7, 32.9, —CH_2—(CH_2)$_{12}$—, 35.6 C—CH_2—NH—, 37.0 CO—CH_2—CH_2, 61.8, 62.6, 76.9, 77.1, 79.6, 80.1,C3′,*C4′*, *C5′*,*C6′*, *C5*, *C6*, 70.4 *C4*, 72.6 *C2*, 73.8 *C2′*, 75.0 *C3*, 89.1 *C1′*, 105.2 *C1*, 123.4 *C*H triazole, 146.4 *C* triazole, 176.2 NH—*C*O—CH$_2$.

MicroTOF MS: 661.4008 [M+ Na]$^+$, calcd: 661.4018.

Anal. calcd for $C_{31}H_{56}N_4O_{11}\bullet H_2O$: C, 54.85; H, 8.61; N, 8.25. Found: C, 55.34; H, 8.96; N, 8.39.

IR (KBr, cm^{-1}): 3328, 2915, 2848, 1649, 1542, 1467, 1416, 1379, 1329, 1247, 1227, 1130, 1089, 1074, 1048, 998, 895, 758, 700, 645.

Cell-Tz-C_{16} $C_{31}H_{56}N_4O_{11}$. ^{1}H NMR (500 MHz, MeOD, 50 °C, δ ppm): 0.90 (t, 3H, *J* = 6.8 Hz, —(CH_2)$_{12}$—*C*H_3), 1.13−1.45 (m, 24H, —(*C*H_2)$_{12}$—CH_3), 1.56−1.66 (m, 2H, CO—CH_2—*C*H_2—(CH_2)$_{12}$), 2.21 (t, 2H, *J* = 7.3 Hz, CO—*C*H_2—CH_2), 3.27 (dd, 1H, $J_{1,2}$ = 7.3 Hz, $J_{2,3}$ = 8.4 Hz, *H2*), 3.32−3.46 (m, 3H), 3.65−3.80 (m, 4H), 3.85−3.92 (m, 3H, *H3′*, *H4′*, *H5′*, *H6′a*, *H6′b*, *H3*, *H4*, *H5*, *H6a*, *H6b*), 3.95 (dd, 1H, $J_{1',2'}$ = 9.8 Hz, $J_{2',3'}$ = 7.7 Hz, *H2′*), 4.45 (m, 2H, C—CH_2—NH), 4.48 (d, 1H, $J_{1,2}$ = 7.3 Hz, *H1*), 5.60 (d, 1H, $J_{1',2'}$ = 9.2 Hz, *H1′*), 8.00 (s, 1H, C*H* triazole).

^{13}C NMR (125 MHz, MeOD, 55 °C, δ ppm): 14.3 —(CH_2)$_{12}$—*C*H_3, 23.6 —(CH_2)$_{12}$—, 26.8 CO—CH_2—CH_2—(CH_2)$_{12}$, 30.4, 30.5, 30.7, 32.9 —CH_2—(CH_2)$_{12}$—, 35.6 C—CH_2—NH—, 37.0 CO—*C*H_2—CH_2, 61.7, 62.6, 71.5, 76.9, 78.0, 78.2, 79.6, 79.9 *C3′*,*C4′*, *C5′*,*C6′*, *C3*,*C4*, *C5*,*C6*, 73.8 *C2′*, 75.6 *C2*, 89.4 *C1′*, 104.6 *C1*, 123.4 *C*H triazole, 146.4 *C* triazole, 176.3 NH—*C*O—CH$_2$.

MicroTOF MS: 661.3997 [M+ H]$^+$, calcd: 661.4018.

Anal. calcd for $C_{31}H_{56}N_4O_{11}\bullet H_2O$: C, 54.85; H, 8.61; N, 8.25. Found: C, 54.94; H, 8.88; N, 8.27.

IR (KBr, cm^{-1}): 3326, 2915, 2848, 1649, 1542, 1468, 1368, 1328, 1247, 1227, 1210, 1095, 1041, 997, 899, 997, 899, 831, 760, 719, 655.

Characterization Techniques. ^{1}H and ^{13}C NMR spectra were recorded on BRUKER AV-400 or AV-500 spectrometers. IR spectra were measured on Thermo NICOLET Avatar 360 FT-IR spectrophotometer using KBr pellets. Mass Analysis was performed using a MALDI+/TOF Brüker Microflex system with a DIT + NaFTA matrix and MicroTOF Brüker equipment for exact mass measurements. Elemental analysis was performed using a Perkin-Elmer CHN2400 microanalyzer.

The mesogenic behavior was studied by optical microscopy with an Olympus BH-2 polarizing microscope equipped with a Linkam THMS hot-stage central processor and a CS196 cooling system. Differential scanning calorimetry (DSC) was performed using a DSC Q2000 from TA Instruments with samples sealed in aluminum pans and a scanning rate of 10 °C/min under a nitrogen atmosphere. Temperatures were read at the maximum of the transition peaks and glass transition at the midpoint of the jump of the baseline. Thermogravimetric analysis (TGA) was performed using a TGA Q5000IR from TA Instruments at a rate of 10 °C/min under a nitrogen atmosphere. Circular dichroism was measured using a Jasco J-180 equipment. The CD spectra of the samples were registered by rotating the sandwich every 60 degrees around the light beam axis.

FESEM measurements were performed using a Carl Zeiss MERLIN equipment at the laboratory of the 'Servicio de Microscopia de la Universidad de Zaragoza'. The sample was fixed onto glass and coated with platinum. ESEM measurements were performed using a QUANTA FEG 250 and TEM measurements were performed using a TECNAI G^2 20 (FEI COMPANY), 200 kV, both at the Laboratory of Advanced Microscopy (LMA) of the 'Instituto de Nanociencia de Aragon'. For TEM sample preparation, a drop of the solution (gel diluted) was placed on a copper grid and left to dry for 15 min. The copper grid was then placed again over a drop of 1% uranyl acetate solution as a negative stain for 30 s and was then left to dry. CryoTEM measurements were performed on this microscope with a cryo-holder.

AFM measurements were performed using a VEECO MULTI-MODE 8, mode tapping and tips 20−80 nN/m and υ 300 kHz at Laboratory of Advanced Microscopy (LMA).

Gelation test: The gelator and the solvent were placed in a septum-capped test tube. The resulting mixture was heated until a clear solution was obtained. The solution was cooled to room temperature and if the tube was turned upside down and the solution did not flow, the formation of a gel was registered.

■ ASSOCIATED CONTENT

Ⓢ Supporting Information

^{1}H NMR of OAc-Lact-Tz-C_{16} and Lact-Tz-C_{16}. Thermogravimetric analysis of peracetylated precursors and glycolipids. Microphotograph of Cell-Tz-C_{16} by POM. DSC curves in the solid state of Cell-Tz-C_{16} and Lact-Tz-C_{16}. X-ray patterns of Cell-Tz-C_{16}. DSC analysis of Cell-Tz-C_{16} (0.5 wt %) water gel. ^{1}H NMR spectra of Cell-Tz-C_{16} hydrogel, 0.5 wt % D_2O, taken at different temperatures. ^{1}H NMR spectra of Lact-Tz-C_{16} hydrogel, 1 wt % D_2O, taken at different temperatures. ^{1}H NMR experiments in DMSO-d_6 increasing water concentration of Cell-Tz-C_{16}. ESEM images of Lact-Tz-C_{16} (1 wt % water) gel decreasing humidity. CryoTEM images of Cell-Tz-C_{16} (0.5 wt %) water gel and Lact-Tz-C_{16} (1 wt %) water gel. CD and UV−vis spectra of hydrogels derived from Cell-Tz-C_{16} and Lact-Tz-C_{16} at 1 wt %. This material is available free of charge via the Internet at http://pubs.acs.org.

■ AUTHOR INFORMATION

Corresponding Author

*E-mail: loriol@unizar.es and fitremann@chimie.ups-tlse.fr.

dx.doi.org/10.1021/cm301509v | *Chem. Mater.* XXXX, XXX, XXX−XXX

Notes

The authors declare no competing financial interest.

■ ACKNOWLEDGMENTS

Financial support from the Spanish MINECO project MAT2011-27978-C02-01, Fondo Europeo de Desarrollo Regional (FEDER), and Gobierno de Aragón, and Fondo Social Europeo is gratefully acknowledged. The authors also acknowledge 'Servicio de Microscopia de la Universidad de Zaragoza' for FESEM measurements, Laboratory of Advanced Microscopy (LMA) of the INA (Instituto de Nanociencia de Aragón) for ESEM, and AFM measurements and Dr. Emma Cavero for TEM and cryo-TEM measurements.

■ REFERENCES

(1) Estroff, L. A.; Hamilton, A. D. *Chem. Rev.* **2004**, *104*, 1201.
(2) (a) Terech, P.; Weiss, R. G. *Chem. Rev.* **1997**, *97*, 3133. (b) Abdallah, D. J.; Weiss, R. G. *Adv. Mater.* **2000**, *12*, 1237. (c) Ajayaghosh, A.; Praveen, V. K.; Vijayakumar, C. *Chem. Soc. Rev.* **2008**, *37*, 109. (d) Banerjee, S.; Das, R. K.; Maitra, U. *J. Mater. Chem.* **2009**, *19*, 6649. (e) Smith, D. K. *Chem. Soc. Rev.* **2009**, *38*, 684.
(3) Sangeetha, N. M.; Maitra, U. *Chem. Soc. Rev.* **2005**, *34*, 821.
(4) Hirst, A. R.; Escuder, B.; Miravet, J. F.; Smith, D. K. *Angew. Chem., Int. Ed.* **2008**, *47*, 8002.
(5) (a) Kiyonaka, S.; Sugiyasu, K.; Shinkai, S.; Hamachi, I. *J. Am. Chem. Soc.* **2002**, *124*, 10954. (b) Kiyonaka, S.; Sada, K.; Yoshimura, I.; Shinkai, S.; Kato, N.; Hamachi, I. *Nat. Mater.* **2004**, *3*, 58. (c) Yoshimura, I.; Miyahara, Y.; Kasagi, N.; Yamane, H.; Ojida, A.; Hamachi, I. *J. Am. Chem. Soc.* **2004**, *126*, 12204. (d) Tamaru, S.; Kiyonaka, S.; Hamachi, I. *Chem.—Eur. J.* **2005**, *11*, 7294. (e) Yamaguchi, S.; Yoshimura, L.; Kohira, T.; Tamaru, S.; Hamachi, I. *J. Am. Chem. Soc.* **2005**, *127*, 11835. (f) Koshi, Y.; Nakata, E.; Yamane, H.; Hamachi, I. *J. Am. Chem. Soc.* **2006**, *128*, 10413. (g) Matsumoto, S.; Yamaguchi, S.; Ueno, S.; Komatsu, H.; Ikeda, M.; Ishizuka, K.; Iko, Y.; Tabata, K. V.; Aoki, H.; Ito, S.; Noji, H.; Hamachi, I. *Chem.—Eur. J.* **2008**, *14*, 3977. (h) Matsumoto, S.; Yamaguchi, S.; Wada, A.; Matsui, T.; Ikeda, M.; Hamachi, I. *Chem. Commun.* **2008**, *13*, 1545.
(6) (a) Ikeda, M.; Ueno, S.; Matsumoto, S.; Shimizu, Y.; Komatsu, H.; Kusumoto, K. I.; Hamachi, I. *Chem.—Eur. J.* **2008**, *14*, 10808. (b) Wang, W. J.; Wang, H. M.; Ren, C. H.; Wang, J. Y.; Tan, M.; Shen, J.; Yang, Z. M.; Wang, P. G.; Wang, L. *Carbohydr. Res.* **2011**, *346*, 1013.
(7) (a) Pfannemuller, B.; Welte, W. *Chem. Phys. Lipids* **1985**, *37*, 227. (b) Fuhrhop, J. H.; Schnieder, P.; Rosenberg, J.; Boekema, E. *J. Am. Chem. Soc.* **1987**, *109*, 3387. (c) Fuhrhop, J. H.; Schnieder, P.; Boekema, E.; Helfrich, W. *J. Am. Chem. Soc.* **1988**, *110*, 2861.
(8) (a) John, G.; Masuda, M.; Okada, Y.; Yase, K.; Shimizu, T. *Adv. Mater.* **2001**, *13*, 715. (b) Jung, J. H.; John, G.; Masuda, M.; Yoshida, K.; Shinkai, S.; Shimizu, T. *Langmuir* **2001**, *17*, 7229. (c) Yang, Z. M.; Liang, G. L.; Ma, M. L.; Abbah, A. S.; Lu, W. W.; Xu, B. *Chem. Commun.* **2007**, *8*, 843.
(9) (a) Shimizu, T.; Masuda, M. *J. Am. Chem. Soc.* **1997**, *119*, 2812. (b) Jung, J. H.; Shinkai, S.; Shimizu, T. *Chem.—Eur. J.* **2002**, *8*, 2684. (c) Shimizu, T. *Pol. J.* **2003**, *35*, 1.
(10) (a) Bhattacharya, S.; Maitra, U.; Mukhopadhyay, S.; Srivastava, A. Advances in molecular hydrogels. In *Molecular Gels*; Weiss, R. G., Terech, P., Eds., Springer: Dordrecht, 2006, p 628; (b) Srivastava, A.; Ghorai, S.; Bhattacharjya, A.; Bhattacharya, S. *J. Org. Chem.* **2005**, *70*, 6574.
(11) (a) Hamachi, I.; Kiyonaka, S.; Shinkai, S. *Chem. Commun.* **2000**, *14*, 1281. (b) Kiyonaka, S.; Shinkai, S.; Hamachi, I. *Chem.—Eur. J.* **2003**, *9*, 976. (c) Mohan, S. R. K.; Hamachi, I. *Curr. Org. Chem.* **2005**, *9*, 491.
(12) Bhattacharya, S.; Acharya, S. N. G. *Chem. Mater.* **1999**, *11*, 3504.
(13) Goodby, J. W.; Gortz, V.; Cowling, S. J.; Mackenzie, G.; Martin, P.; Plusquellec, D.; Benvegnu, T.; Boullanger, P.; Lafont, D.; Queneau, Y.; Chambert, S.; Fitremann, J. *Chem. Soc. Rev.* **2007**, *36*, 1971.
(14) (a) Dorset, D. L.; Rosenbusch, J. P. *Chem. Phys. Lipids* **1981**, *29*, 299. (b) Goodby, J. W. *Mol. Cryst. Liq. Cryst.* **1984**, *110*, 205. (c) Miethchen, R.; Holz, J.; Prade, H.; Liptak, A. *Tetrahedron* **1992**, *48*, 3061.
(15) (a) Fischer, S.; Fischer, H.; Diele, S.; Pelzl, G.; Jankowski, K.; Schmidt, R. R.; Vill, V. *Liq. Cryst.* **1994**, *17*, 855. (b) Molinier, V.; Kouwer, P. H. J.; Fitremann, J.; Bouchu, A.; Mackenzie, G.; Queneau, Y.; Goodby, J. W. *Chem.—Eur. J.* **2006**, *12*, 3547. (c) Queneau, Y.; Gagnaire, J.; West, J. J.; Mackenzie, G.; Goodby, J. W. *J. Mater. Chem.* **2001**, *11*, 2839.
(16) (a) Auvray, X.; Petipas, C.; Anthore, R.; Rico-Lattes, I.; Lattes, A. *Langmuir* **1995**, *11*, 433. (b) Goodby, J. W.; Haley, J. A.; Mackenzie, G.; Watson, M. J.; Plusquellec, D.; Ferrieres, V. *J. Mater. Chem.* **1995**, *5*, 2209. (c) Ho, M. S.; Hsu, C. S. *Liq. Cryst.* **2010**, *37*, 293. (d) Smits, E.; Engberts, J.; Kellogg, R. M.; VanDoren, H. A. *Liq. Cryst.* **1997**, *23*, 481. (e) Vandoren, H. A.; Vandergeest, R.; Deruijter, C. F.; Kellogg, R. M.; Wynberg, H. *Liq. Cryst.* **1990**, *8*, 109.
(17) (a) Gerber, S.; Wulf, M.; Milkereit, G.; Vill, V.; Howe, J.; Roessle, M.; Garidel, P.; Gutsmann, T.; Brandenburg, K. *Chem. Phys. Lipids* **2009**, *158*, 118. (b) Ma, Y. D.; Takada, A.; Sugiura, M.; Fukuda, T.; Miyamoto, T.; Watanabe, J. *Bull. Chem. Soc. Jpn.* **1994**, *67*, 346. (c) von Minden, H. M.; Brandenburg, K.; Seydel, U.; Koch, M. H. J.; Garamus, V.; Willumeit, R.; Vill, V. *Chem. Phys. Lipids* **2000**, *106*, 157.
(18) Clemente, M. J.; Fitremann, J.; Mauzac, M.; Serrano, J. L.; Oriol, L. *Langmuir* **2011**, *27*, 15236.
(19) (a) Kolb, H. C.; Finn, M. G.; Sharpless, K. B. *Angew. Chem., Int. Ed.* **2001**, *40*, 2004. (b) Tornoe, C. W.; Christensen, C.; Meldal, M. *J. Org. Chem.* **2002**, *67*, 3057. (c) Wu, P.; Feldman, A. K.; Nugent, A. K.; Hawker, C. J.; Scheel, A.; Voit, B.; Pyun, J.; Frechet, J. M. J.; Sharpless, K. B.; Fokin, V. V. *Angew. Chem., Int. Ed.* **2004**, *43*, 3928.
(20) Juwarker, H.; Lenhardt, J. M.; Castillo, J. C.; Zhao, E.; Krishnamurthy, S.; Jamiolkowski, R. M.; Kim, K. H.; Craig, S. L. *J. Org. Chem.* **2009**, *74*, 8924.
(21) (a) da Silva, C. O.; Nascimento, M. A. C. *Carbohydr. Res.* **2004**, *339*, 113. (b) Momany, F. A.; Schnupf, U.; Willett, J. L.; Bosma, W. B. *Struct. Chem.* **2007**, *18*, 611. (c) French, A. D.; Johnson, G. P.; Cramer, C. J.; Csonka, G. I. *Carbohydr. Res.* **2012**, *350*, 68.
(22) Bhattacharya, S.; Acharya, S. N. G. *Langmuir* **2000**, *16*, 87.
(23) (a) Gyorgydeak, Z.; Szilagyi, L.; Paulsen, H. *J. Carbohydr. Chem.* **1993**, *12*, 139. (b) Bianchi, A.; Bernardi, A. *J. Org. Chem.* **2006**, *71*, 4565.
(24) (a) Suzuki, M.; Yumoto, M.; Kimura, M.; Shirai, H.; Hanabusa, K. *Chem.—Eur. J.* **2003**, *9*, 348. (b) Ikeda, M.; Nobori, T.; Schmutz, M.; Lehn, J. M. *Chem.—Eur. J.* **2005**, *11*, 662.
(25) Park, J.; Rader, L. H.; Thomas, G. B.; Danoff, E. J.; English, D. S.; DeShong, P. *Soft Matter* **2008**, *4*, 1916.